ChemPubSoc Europe

DOI: 10.1002/cphc.201601227

CHEMPHYSCHEM Communications

Separation of Anti-Phase Signals Due to Parahydrogen Induced Polarization via 2D Nutation NMR Spectroscopy

Utz Obenaus,[a] Gerhard Althoff-Ospelt,[b] Swen Lang,[a] Robin Himmelmann,[a] and Michael Hunger*[a]

The present work introduces a novel method for the selective detection of ^{1}H NMR *anti*-phase signals caused by the pairwise incorporation of parahydrogen into olefins on noble-metal-containing catalysts. Via a two-dimensional (2D) nutation NMR experiment, the *anti*-phase signals of hyperpolarized ^{1}H nuclei are separated due to their double nutation frequency compared to that of thermally polarized ^{1}H nuclei. For demonstrating this approach, parahydrogen induced polarization (PHIP) was achieved via the hydrogenation of propene with parahydrogen on platinum-containing silica and investigated by in situ ^{1}H MAS NMR spectroscopy under continuous-flow conditions, that is, the hydrogenation reaction was performed inside the magnet of the NMR spectrometer. The 2D nutation NMR experiment described in the present work is useful for the separation of overlapping *anti*-phase and *in*-phase signals due to hyperpolarized and thermally polarized ^{1}H nuclei, respectively, which is important for research in the field of heterogeneous catalysis.

The heterogeneously catalyzed hydrogenation of hydrocarbons is an important reaction in petrochemistry and refining. Examples are the selective conversion of double- and triple-bond-containing organic compounds with and without functional groups into desired products, the purification of feedstocks for polymerization reactions from polyenes, which are poisoning the polymerization catalysts, and the elimination of alkynes in gas streams of alkenes.[1–4] In the past decades, in situ solid-state NMR spectroscopy under flow conditions has demonstrated an increasing potential for investigating the mechanisms of heterogeneously catalyzed reactions.[5] Broad application of this method, however, requires an enhancement of the sensitivity for the detection of intermediates and active surface sites. An interesting strategy for enhancing the sensitivity of NMR spectroscopy for the investigation of heterogeneously catalyzed reaction systems is the coupling of the nuclear spins under study to a reservoir of nuclei with much higher polarization.[6] A suitable route is the pairwise incorporation of the two hydrogen atoms of parahydrogen molecules into olefins leading to reaction products with parahydrogen induced polarization.[7–9] In this case, a large non-equilibrium spin polarization, that is, a hyperpolarization, may occur. Normal hydrogen gas (assigned n-H_2 in this work) has a *para* (nuclear spin $I=0$) to *ortho* (nuclear spin $I=1$) ratio of 1:3, which can be converted to a *para* to *ortho* ratio of 1:1 (assigned p-H_2 in this work) by contacting n-H_2 with activated charcoal or iron oxide at 77 K.[9,10] The PASADENA (Parahydrogen And Synthesis Allow Dramatically Enhanced Nuclear Alignment) protocol applied in the present work is based on the hydrogenation of olefins with p-H_2 inside the magnet of the NMR spectrometer. In the ^{1}H NMR spectra of the reactants, this procedure is accompanied by an appearance of characteristic *anti*-phase signals, which are due to a pairwise incorporation of the hydrogen atoms of p-H_2 into the olefin molecules.[9–14] In comparison with the ^{1}H NMR signals caused by the hydrogenation of the same olefin molecules with n-H_2, the above-mentioned *anti*-phase signals can show an intensity enhancement by up to three orders of magnitude due to the PHIP effect.[9]

In the past decade, an increasing number of groups utilized heterogeneously catalyzed hydrogenation reactions for the investigation of PHIP effects.[15–19] Some studies had the aim to form hyperpolarized propane via the heterogeneously catalyzed hydrogenation of propene for applications in the field of magnetic resonance imaging (MRI).[20–22] Furthermore, the progress in the formation of PHIP via heterogeneously catalyzed hydrogenation reactions allowed investigations of reaction mechanisms.[23–27] In all these studies, the NMR detection of the hyperpolarized reaction products was performed by investigating fluid reactant phases. NMR studies of hyperpolarized reaction products interacting with the pore walls or the particle surfaces of solid catalysts, on the other hand, require the application of high-resolution solid-state NMR techniques, such as magic angle spinning (MAS), as done in the present work.

Especially for porous solids, rapid relaxation of the PHIP of nuclei in the reaction products (in this work called hyperpolarized nuclei) on the particle surface and inside the pores may occur. This relaxation can lead to intensities of the *anti*-phase NMR signals of hyperpolarized ^{1}H nuclei comparable to those of the *in*-phase NMR signals of thermally polarized ^{1}H nuclei. In this case, it would be useful to have an experimental technique available, which allows the separation of *anti*-phase signals and *in*-phase signals. The present work demonstrates that such a signal separation is possible along the second dimen-

[a] U. Obenaus, S. Lang, R. Himmelmann, Prof. Dr. M. Hunger
Institute of Chemical Technology
University of Stuttgart
70550 Stuttgart (Germany)
E-mail: michael.hunger@itc.uni-stuttgart.de

[b] Dr. G. Althoff-Ospelt
Solid-State NMR Application
Bruker BioSpin GmbH
Silberstreifen 4, 76287 Rheinstetten (Germany)

Supporting Information and the ORCID identification number(s) for the author(s) of this article can be found under http://dx.doi.org/10.1002/cphc.201601227.

© 2017 Wiley-VCH Verlag GmbH & Co. KGaA, Weinheim

sion of 2D nutation NMR spectra. This approach is based on the specific properties of hyperpolarized nuclei giving maximum signal intensities after excitation with a $\pi/4$ pulse in contrast to thermally polarized nuclei requiring excitation by a $\pi/2$ pulse for reaching maximum signal intensities.[28,29] Correspondingly, the nutation frequency ν_1 of hyperpolarized nuclei in the radio frequency (ν_{rf}) field of the excitation pulse is factor two higher compared to that of thermally polarized nuclei. A similar effect is known for quadrupolar nuclei, such as ^{23}Na with a nuclear spin of $I=3/2$, which may occur at sites with significantly different quadrupole frequencies ν_q.[30,31] In this case, 2D nutation NMR experiments were utilized for separating the solid-state NMR signals of quadrupolar nuclei with weak ($\nu_q < \nu_{rf}$) and strong ($\nu_q \gg \nu_{rf}$) quadrupolar interactions along the second dimension (ν_1-axis) of 2D nutation NMR spectra at $\nu_1 = 1\nu_{rf}$ and $\nu_1 = 2\nu_{rf}$, respectively.[32–34]

Similarly to the 2D nutation MAS NMR investigations of quadrupolar nuclei, the present 2D nutation NMR experiments with hyperpolarized ^{1}H nuclei were performed by incrementing the pulse length described by the time domain t_1, while the induction decay is recorded as a function of the time domain t_2 (Figure 1, left). The two-dimensional Fourier-transformation (2D FT) of the data as a function of t_1 and t_2 gives a 2D nutation NMR spectrum with the chemical shifts of the observed signals along the F2-axis and their nutation frequencies ν_1 along the F1-axis (Figure 1, right).

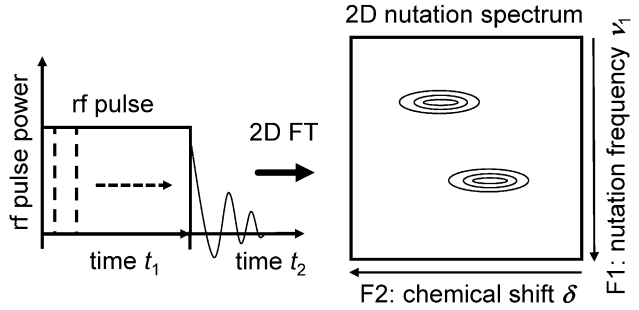

Figure 1. Scheme of the 2D nutation NMR experiment and the nutation spectrum obtained upon 2D Fourier transformation (2D FT) for the time domains t_1 (incremented pulse length) and t_2 (induction decays).

Very recently, first in situ continuous-flow MAS NMR spectroscopic investigations of the formation of PHIP on noble metal-containing solids were performed with the aim to develop novel experimental approaches for mechanistic studies in the field of heterogeneous catalysis.[35,36] In these studies, the hydrogenation of propene with p-H_2 in the gas phase was carried out on solid catalysts filled into a MAS NMR rotor utilized as a spinning micro-reactor. Based on these experiments, the present 2D nutation NMR experiments aiming at the separation of the signals of hyperpolarized and thermally polarized ^{1}H nuclei were performed during in situ hydrogenation of propene with p-H_2 on a platinum-containing silica catalyst (0.9Pt/silica) inside a spinning 4 mm MAS NMR rotor. The 0.9Pt/silica catalyst was prepared and pretreated as described in the Experimental Section. For the hydrogenation of acrylonitrile on this catalyst according to the procedure described in literature,[37] a reaction rate of $(7.6\pm1.1)\times10^{-4}$ mmol s^{-1} was obtained. Under the same conditions, reaction rates of $(2.3\pm0.4)\times10^{-4}$ mmol s^{-1} and $(1.4\pm0.2)\times10^{-3}$ mmol s^{-1} were determined for zeolites 0.8Pt/H,Na-Y and 4.5Pt/H,Na-Y, respectively,[37] which indicate the high hydrogenation activity of the 0.9Pt/silica catalyst utilized in this study.

In the present work, the hydrogenation of propene with p-H_2 on 0.9Pt/silica was performed inside a modified 4 mm MAS NMR rotor spinning with 4 kHz (Figures S1 and S2), with continuous propene and p-H_2 flow rates of 40 and 30 mL min^{-1}, respectively, and at the reaction temperature of 373 K. For experimental details, see Supporting Information. As control experiments, in situ ^{1}H MAS NMR investigations with a fixed single pulse $\pi/4$ excitation, that is, one-dimensional (1D) in situ MAS NMR measurements were performed during the hydrogenation of propene with n-H_2 and p-H_2 leading to the spectra in Figure 2a and Figure 2b, respectively. The spectrum in Figure 2a consists exclusively of signals of thermally polarized ^{1}H nuclei due to propene at 1.3 ± 0.2 ppm, 4.8 ± 0.2 ppm, and 5.6 ± 0.2 ppm and of the reaction product propane at 0.6 ± 0.2 ppm and 1.0 ± 0.2 ppm. Differences between the gas phase chemical shifts in the present work and chemical shifts in the literature[38] are due to the different surroundings of the molecules under study. The additionally observed broad shoulder at 1.6 ± 0.2 ppm is caused by surface OH groups of the silica support.[34] In the spectrum shown in Figure 2b, the signals of thermally polarized ^{1}H nuclei are overlapped by typical *anti*-phase signals due to the pairwise incorporation of p-H_2 into propene. In Figure 2c, the difference spectrum consisting exclusively of the *anti*-phase signals is shown. The chemical shift values of these signals agree with those of propane (0.6 ± 0.2 ppm and 1.0 ± 0.2 ppm).

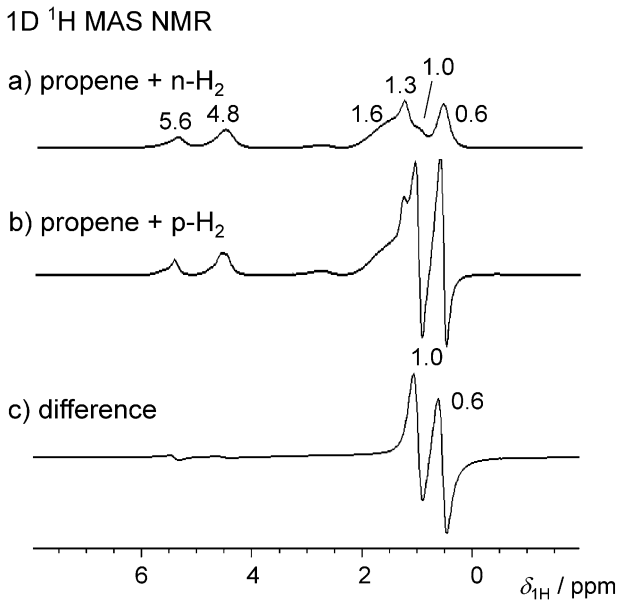

Figure 2. In situ 1D ^{1}H MAS NMR spectra recorded during the hydrogenation of propene with n-H_2 (top) and p-H_2 (middle) on 0.9Pt/silica under continuous-flow conditions at 373 K. The bottom spectrum is the difference of the spectra recorded during hydrogenation with n-H_2 and p-H_2.

© 2017 Wiley-VCH Verlag GmbH & Co. KGaA, Weinheim

The in situ 2D ^{1}H nutation MAS NMR spectra shown in Figures 3 and 4 were recorded with a pulse power of 50 W corresponding a nutation frequency of thermally polarized ^{1}H nuclei of 55 kHz, pulse lengths between 0.1 and 51.3 μs, that is, with 512 increments of 0.1 μs, eight scans per data set, and with a repetition time of D1 = 0.1 s. Measurements with repetition times of up to D1 = 20 s evidenced that no saturation occurs for ^{1}H NMR signals of the continuously flowing (30 and 40 mL min^{-1}) reactants recorded with D1 = 0.1 s.

The in situ 2D ^{1}H nutation MAS NMR spectrum in Figure 3 was recorded during hydrogenation of propene with n-H_2 at 373 K. The slice obtained at $\nu_1 = 1\nu_{rf} = 55$ kHz corresponds to the spectrum that consists of the signals of thermally polarized ^{1}H nuclei (Figure 3, top). Correspondingly, *in*-phase signals of propene at 1.3 ± 0.2, 4.8 ± 0.2, and 5.6 ± 0.2 ppm and of the reaction product propane at 0.6 ± 0.2 and 1.0 ± 0.2 ppm occur. These shift values agree with those observed in the in situ 1D ^{1}H MAS NMR spectrum in Figure 2a. No signals occur for the slice obtained at $\nu_1 = 2\nu_{rf} = 110$ kHz in Figure 3, bottom.

Hydrogenation of propene with p-H_2 on the 0.9Pt/silica catalyst led to the in situ 2D ^{1}H nutation MAS NMR spectrum in Figure 4. Again, the slice at $\nu_1 = 1\nu_{rf} = 55$ kHz corresponds to the spectrum that consists of the *in*-phase signals of thermally polarized ^{1}H nuclei (Figure 4, top). In comparison with the spectrum in Figure 3, top, however, the signals of the reaction product propane at 0.6 ± 0.2 ppm and 1.0 ± 0.2 ppm are much weaker. Instead, the slice of the nutation spectrum at $\nu_1 = 2\nu_{rf} = 110$ kHz (Figure 4, bottom) shows pure *anti*-phase signals of hyperpolarized nuclei at 0.6 ± 0.2 ppm and 1.0 ± 0.2 ppm, caused by a pairwise incorporation of p-H_2 into propene.

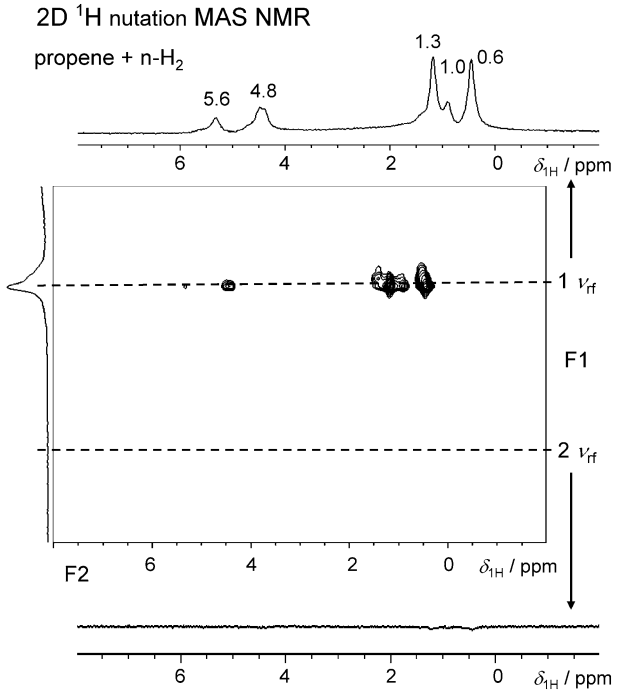

Figure 3. In situ 2D ^{1}H nutation MAS NMR spectrum (middle) recorded during hydrogenation of propene with n-H_2 on 0.9Pt/silica at 373 K and slices of this spectrum at the nutation frequencies of $1\nu_{rf}$ (top) and $2\nu_{rf}$ (bottom).

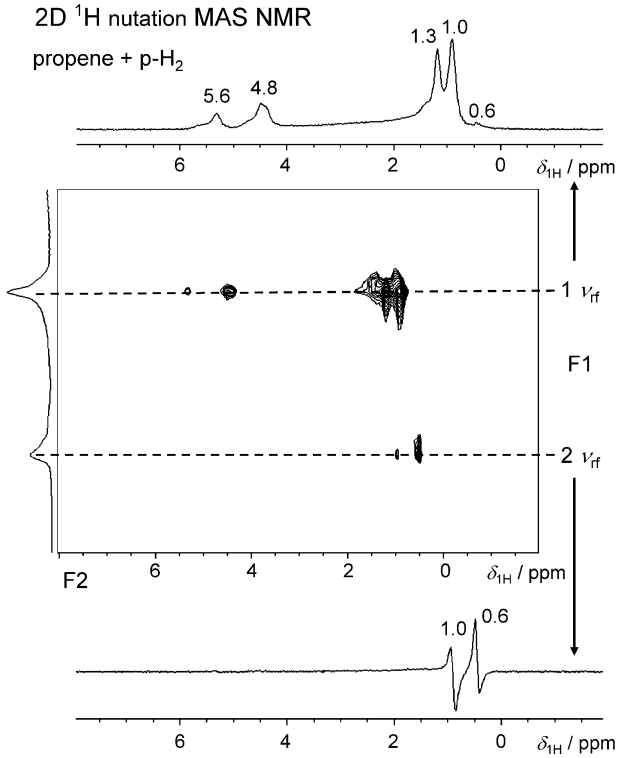

Figure 4. In situ 2D ^{1}H nutation MAS NMR spectrum (middle) recorded during hydrogenation of propene with p-H_2 on 0.9Pt/silica at 373 K and slices of this spectrum at the nutation frequencies of $1\nu_{rf}$ (top) and $2\nu_{rf}$ (bottom).

Hence, by sampling the nutation frequency of thermally polarized and hyperpolarized ^{1}H nuclei during the radio frequency pulse via a 2D NMR experiment, the *in*-phase and *anti*-phase signals of the above-mentioned nuclei are well-separated along the F1 dimension. In future, this new experimental approach allows a more detailed investigation of the formation and relaxation of PHIP of the product molecules of hydrogenation reactions on solid catalysts, especially for the case of overlapping signals of thermally polarized and hyperpolarized nuclei.

Summarizing, the present work demonstrates the possibilities and advantages of 2D nutation NMR spectroscopy for the selective detection of *anti*-phase signals of hyperpolarized ^{1}H nuclei caused by the formation of parahydrogen induced polarization (PHIP) via the PASADENA protocol. This experimental approach, in combination with in situ ^{1}H MAS NMR spectroscopy under continuous-flow conditions, opens novel possibilities for mechanistic studies of heterogeneously catalyzed hydrogenation reactions via PHIP.

Experimental Section

The commercially available silica Aerosil 300 (Degussa AG, Hanau, Germany) was used as delivered. The platinum-containing silica was obtained by stirring 5 g of the silica material in 100 mL of demineralized water at 313 K for 2 h and subsequent addition of 1 M aqueous solution of ammonia until the pH of the reaction solution reached pH 10. Then, an aqueous solution with the calculated

© 2017 Wiley-VCH Verlag GmbH & Co. KGaA, Weinheim

amount of the platinum salt $[Pt(NH_3)_4]Cl_2 \cdot x H_2O$ (55.66 wt% Pt, ChemPur) was added dropwise, and the solution was stirred at 313 K for another 18 h. Finally, this solution was washed with 1.5 L demineralized water and dried under atmospheric conditions at 353 K for 12 h. The obtained sample with the platinum content 0.85 wt% was assigned 0.9Pt/silica. By chemisorption of hydrogen, a noble metal dispersion of $D = 83\%$ was determined. By nitrogen adsorption on dehydrated 0.9Pt/silica, a specific surface area (BET) of 277 $m^2 g^{-1}$, a total pore volume of 0.31 $cm^3 g^{-1}$, and a mean mesopore diameter of 4.5 nm were obtained.

For experimental details of the in situ ^1H MAS NMR experiments, see the Supporting Information.

Acknowledgements

We thank the Deutsche Forschungsgemeinschaft for financial support (project HU533/13-1) and Matthias Scheibe and Heike Fingerle (both University of Stuttgart) for chemisorption experiments and ICP-OES measurements, respectively.

Keywords: heterogeneous catalysis · hydrogenation · NMR spectroscopy · parahydrogen induced polarization · propene

[1] A. Borodzinski, G. C. Bond, *Catal. Rev. Sci. Eng.* **2008**, *50*, 379 – 469.
[2] A. N. R. Bos, G. C. Bond, *Chem. Eng. Process.* **1993**, *32*, 1 – 7.
[3] H. Arnold, F. Doebert, J. Gaube in *Handbook of Heterogeneous Catalysis, 2nd ed.* (Eds.: G. Ertl, H. Knoezinger, F. Schueth, J. Weitkamp), Wiley-VCH, Weinheim, **2008**, pp. 3266 – 3284.
[4] H.-U. Blaser, A. Schnyder, H. Steiner, F. Roessler, P. Baumeister, in *Handbook of Heterogeneous Catalysis, 2nd ed.* (Eds.: G. Ertl, H. Knoezinger, F. Schueth, J. Weitkamp), Wiley-VCH, Weinheim, **2008**, pp. 3284 – 3308.
[5] M. Hunger, *Prog. Nucl. Magn. Reson. Spectrosc.* **2008**, *53*, 105 – 127.
[6] R. G. Griffin, T. F. Prisner, *Phys. Chem. Chem. Phys.* **2010**, *12*, 5737 – 5740.
[7] C. R. Bowers, D. P. Weitekamp, *Phys. Rev. Lett.* **1986**, *57*, 2645 – 2648.
[8] C. R. Bowers, D. P. Weitekamp, *J. Am. Chem. Soc.* **1987**, *109*, 5541 – 5542.
[9] J. Natterer, J. Bargon, *Prog. Nucl. Magn. Reson. Spectrosc.* **1997**, *31*, 293 – 315.
[10] I. V. Skovpin, V. V. Zhivonitko, I. V. Koptyug, *Appl. Magn. Reson.* **2011**, *41*, 393 – 410.
[11] S. B. Duckett, N. J. Wood, *Coord. Chem. Rev.* **2008**, *252*, 2278 – 2291.
[12] I. V. Koptyug, V. V. Zhivonitko, K. V. Kovtunov, *ChemPhysChem* **2010**, *11*, 3086 – 3088.
[13] D. Canet, S. Bouguet-Bonnet, C. Aroulanda, F. Reineri, *J. Am. Chem. Soc.* **2007**, *129*, 1445 – 1449.
[14] P. J. Carson, C. R. Bowers, D. P. Weitekamp, *J. Am. Chem. Soc.* **2001**, *123*, 11821 – 11822.
[15] K. V. Kovtunov, I. E. Beck, V. I. Bukhtiyarov, I. V. Koptyug, *Angew. Chem. Int. Ed.* **2008**, *47*, 1492 – 1495; *Angew. Chem.* **2008**, *120*, 1514 – 1517.
[16] D. A. Barskiy, K. V. Kovtunov, A. Primo, A. Corma, R. Kaptein, I. V. Koptyug, *ChemCatChem* **2012**, *4*, 2031 – 2035.
[17] T. Trantzschel, J. Bernarding, M. Plaumann, D. Lego, T. Gutmann, T. Ratajczyk, S. Dillenberger, G. Buntkowsky, J. Bargon, U. Bommerich, *Phys. Chem. Chem. Phys.* **2012**, *14*, 5601 – 5604.
[18] A. M. Balu, S. B. Duckett, R. Luque, *Dalton Trans.* **2009**, 5074 – 5076.
[19] R. Zhou, E. W. Zhao, W. Cheng, L. M. Neal, H. Zheng, R. E. Quiñones, H. E. Hagelin-Weaver, C. R. Bowers, *J. Am. Chem. Soc.* **2015**, *137*, 1938 – 1946.
[20] L.-S. Bouchard, K. V. Kovtunov, S. R. Burt, M. S. Anwar, I. V. Koptyug, R. Z. Sagdeev, A. Pines, *Angew. Chem. Int. Ed.* **2007**, *46*, 4064 – 4068; *Angew. Chem.* **2007**, *119*, 4142 – 4146.
[21] L.-S. Bouchard, S. R. Burt, M. S. Anwar, K. V. Kovtunov, I. V. Koptyug, A. Pines, *Science* **2008**, *319*, 442 – 445.
[22] K. V. Kovtunov, D. A. Barskiy, A. M. Coffey, M. L. Truong, O. G. Salnikov, A. K. Khudorozhkov, E. A. Inozemtseva, I. P. Prosvirin, V. I. Bukhtiyarov, K. W. Waddell, E. Y. Chekmenev, I. V. Koptyug, *Chem. Eur. J.* **2014**, *20*, 11636 – 11639.
[23] K. V. Kovtunov, D. A. Barskiy, O. G. Salnikov, D. B. Burueva, A. K. Khudorozhkov, A. V. Bukhtiyarov, I. P. Prosvirin, E. Y. Gerasimov, V. I. Bukhtiyarov, I. V. Koptyug, *ChemCatChem* **2015**, *7*, 2581 – 2584.
[24] D. B. Burueva, O. G. Salnikov, K. V. Kovtunov, A. S. Romanov, L. M. Kovtunova, A. K. Khudorozhkov, A. V. Bukhtiyarov, I. P. Prosvirin, V. I. Bukhtiyarov, I. V. Koptyug, *J. Phys. Chem. C* **2016**, *120*, 13541 – 13548.
[25] O. G. Salnikov, K. V. Kovtunov, D. A. Barskiy, A. K. Khudorozhkov, E. A. Inozemtseva, I. P. Prosvirin, V. I. Bukhtiyarov, I. V. Koptyug, *ACS Catal.* **2014**, *4*, 2022 – 2028.
[26] E. Zhao, H. Zheng, K. Ludden, Y. Xin, H. E. Hagelin-Weaver, C. R. Bowers, *ACS Catal.* **2016**, *6*, 974 – 978.
[27] R. Zhou, W. Cheng, L. M. Neal, E. W. Zhao, H. B. Zheng, H. E. Hagelin-Weaver, C. R. Bowers, *Phys. Chem. Chem. Phys.* **2015**, *17*, 26121 – 26129.
[28] D. Canet, *Nuclear Magnetic Resonance: Concepts and Methods, 1st ed.*, John Wiley & Sons, New York, **1996**.
[29] D. Canet, C. Aroulanda, P. Mutzenhardt, S. Aime, R. Gobetto, F. Reineri, *Concepts in Magnetic Resonance A* **2006**, *28*, 321 – 330.
[30] D. Fenzke, D. Freude, T. Froehlich, J. Haase, *Chem. Phys. Lett.* **1984**, *111*, 171 – 175.
[31] A. P. M. Kentgens, J. J. M. Lemmens, F. M. M. Guerts, W. S. Veeman, *J. Magn. Reson.* **1987**, *71*, 62 – 74.
[32] G. A. H. Tijink, R. Janssen, W. S. Veeman, *J. Am. Chem. Soc.* **1987**, *109*, 7301 – 7303.
[33] C.-F. Lin, K.-J. Chao, *J. Phys. Chem.* **1991**, *95*, 9411 – 9414.
[34] M. Hunger, G. Engelhardt, H. Koller, J. Weitkamp, *Solid State Nucl. Magn. Reson.* **1993**, *2*, 111 – 120.
[35] H. Henning, M. Dyballa, M. Scheibe, E. Klemm, M. Hunger, *Chem. Phys. Lett.* **2013**, *555*, 258 – 262.
[36] S. S. Arzumanov, A. G. Stepanov, *J. Phys. Chem. C* **2013**, *117*, 2888 – 2892.
[37] U. Obenaus, F. Neher, M. Scheibe, M. Dyballa, S. Lang, M. Hunger, *J. Phys. Chem. C* **2016**, *120*, 2284 – 2291.
[38] M. Hesse, H. Meier, B. Zeeh, *Spektroskopische Methoden in der organischen Chemie, 8th ed.*, Georg Thieme Verlag KG, Stuttgart, **2012**, pp. 229 – 247.

Manuscript received: November 9, 2016
Revised: December 15, 2016
Final Article published: January 23, 2017

© 2017 Wiley-VCH Verlag GmbH & Co. KGaA, Weinheim